Large scale SiC/SiO_x nanocables: Synthesis, photoluminescence, and field emission properties

X. J. Wang, J. F. Tian, L. H. Bao, C. Hui, T. Z. Yang, C. M. Shen, and H.-J. Gao[a)]
Beijing National Laboratory for Condensed Matter Physics, Chinese Academy of Sciences, Beijing 100080, People's Republic of China and Institute of Physics, Chinese Academy of Sciences, Beijing 100080, People's Republic of China

F. Liu and N. S. Xu
Guangdong Province Key Laboratory of Display Material and Technology, Sun Yat-Sen University, Guangzhou 510275, People's Republic of China

(Received 6 March 2007; accepted 11 May 2007; published online 13 July 2007)

Large scale, high yield SiC/SiO_x nanocables have been synthesized by thermal evaporation of carbon powders and silicon powders in the presence of Fe_3O_4 nanoparticle catalysts. Transmission electron microscopy and high-resolution transmission electron microscopy show that the nanocables consist of a 50–300 nm single-crystalline β-SiC core wrapped with a 10–20 nm amorphous SiO_x shell. The nanocables have two broad photoluminescence peaks located around 390 and 460 nm when the 250 nm ultraviolet fluorescent light excitation is applied at room temperature. The results of field emission measurement of SiC/SiO_x nanocables indicate the low turn-on and threshold electric fields of 3.2 and 5.3 V/μm at the vacuum gap of 200 μm, respectively. When the vacuum gap was increased to 1000 μm, the turn-on and threshold electric fields were decreased to 1.1 and 2.3 V/μm, respectively. The SiC/SiO_x nanocables with good photoluminescence and field emission properties are promising candidates for ultraviolet-blue emitting devices, flat panel displays, and semiconductor field emitters. © *2007 American Institute of Physics*. [DOI: 10.1063/1.2749474]

I. INTRODUCTION

Research on one-dimensional nanomaterials is at present attracting considerable interest due to its contribution to the understanding of basic concepts as well as potential technological applications.[1,2] Among the various interesting materials, SiC is a semiconductor with an especially wide band as well as other superior properties, such as low density, high hardness and strength, good thermal conductivity, and excellent physical and chemical stabilities.[3,4] The SiC nanowires have been shown to exhibit properties superior to bulk SiC materials. For example, both the elasticity and strength of SiC nanowires are considerably greater than those of micrometer-size SiC whiskers and bulk SiC.[5] Recently, field emission (FE) properties of SiC nanowires and SiC/SiO_x nanocables have been measured, and the results show low turn-on and threshold electric field values.[6,7] The SiC nanowires and SiC/SiO_x nanocables are thus suitable for functional ceramics, high-temperature semiconductors, and electron field-emitting devices due to their excellent mechanical and field emission properties.

The SiC nanowires and SiC/SiO_x nanocables have been synthesized by several techniques, including chemical vapor deposition (CVD),[8–18] physical vapor deposition (PVD),[19] and arc discharge process.[20,21] CVD is a widely used technique to fabricate SiC nanowires and SiC/SiO_x nanocables using carbon nanotubes as the templates to react with SiO or Si,[8–10] and using $SiCl_4$ and CCl_4 as the reactants and metal Na as the coreluctant.[11] This process utilizes the vapor-liquid-solid (VLS) growth mechanism to synthesize the SiC nanowires[7,12–14] and one-dimensional SiC nanostructure without any catalysts.[15–18] However, the above-mentioned methods need to be operated at higher temperature and the synthesis processes are complex. Because of this, synthesis of large scale, high yield SiC nanowires and SiC/SiO_x nanocables remains difficult, which limits further study and applications in many fields.

In this paper, we report a low cost and simple chemical vapor deposition method for fabricating high yield SiC/SiO_x nanocables, which uses the thermal evaporation of silicon powders and carbon powders in the presence of Fe_3O_4 nanoparticle catalysts. Photoluminescence (PL) and field emission properties of SiC/SiO_x nanocables fabricated with this method have been measured, in order to examine the possibility of applications in semiconductor lasers and field emitters as well as in other areas.

II. EXPERIMENT

Fe_3O_4 nanoparticles with a diameter less than 10 nm were synthesized by high-temperature solution phase reaction of iron (III) acetylacetonate with 1,2-dodecanediol in the presence of oleic acid and oleylamine.[22] The growth of SiC/SiO_x nanocables was conducted in a horizontal tube furnace with a quartz tube. A ceramic boat was charged with 0.2 g carbon powders (99.9%) and placed at the center of the furnace. The Fe_3O_4 liquid drops were spread over Si(111) wafer surface, followed by immerging a small amount of silicon powders (99.9%) into these liquid drops. The coated Si(111) wafer was placed above another ceramic boat as the substrate, which was located at the front of first ceramic boat

[a)]Author to whom correspondence should be addressed; electronic mail: hjgao@aphy.iphy.ac.cn

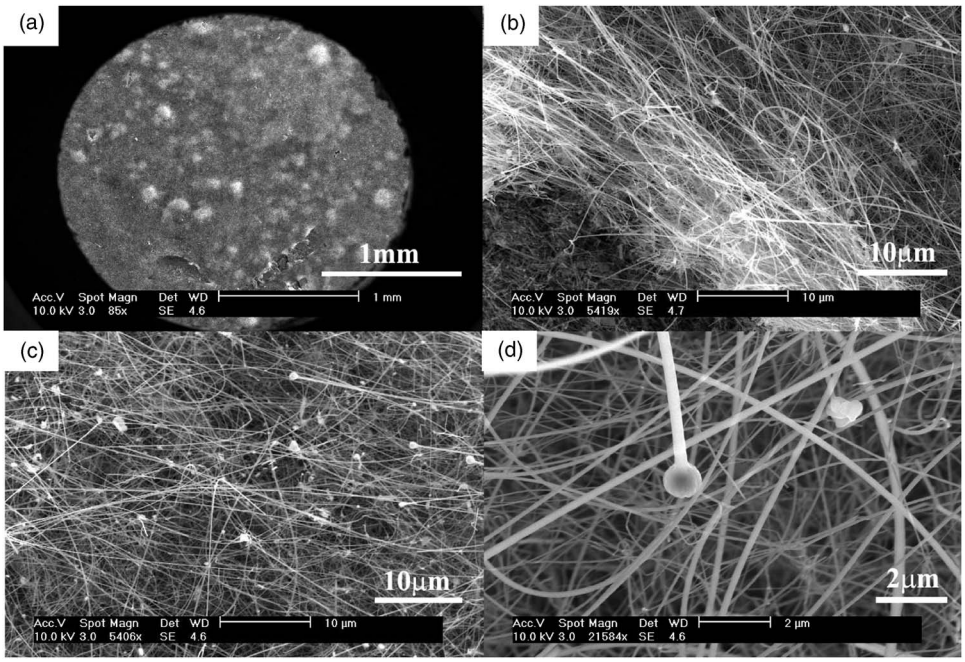

FIG. 1. SEM images of SiC/SiO_x nanocables deposited on the Si(111) substrate at the reaction temperature of 1000 °C for 2 h. (a) Low magnification SEM image of nanocables. [(b)–(d)] High magnification SEM images of nanocables.

loaded with carbon powders. Prior to heating, the system was flushed with high-purity Ar at a constant flow rate of 300 SCCM (SCCM denotes cubic centimeter per minute at STP) for 30 min. The SiC/SiO_x nanocables were grown using a two-step furnace profile. In the first step, the furnace was raised to 400 °C and held for 30 min to eliminate the remained oleic acid and oleylamine. This was followed by raising the furnace temperature to 1000 °C and lowering the Ar flow rate to 50 SCCM, allowing the growth of SiC/SiO_x nanocables. During the above process, the gas pressure in the quartz tube was maintained at 5×10^3 Pa. After 2 h, the furnace was cooled to room temperature in Ar atmosphere, and the white product was found on the surface of Si(111) substrate.

Field emission scanning electron microscope (FESEM) (XL-SFEG, FEI Corp.) was used for the morphological observation of SiC/SiO_x nanocables. X-ray diffraction (XRD) (D/Max-2400, Rigaku Corp.) with Cu $K\alpha$ radiation was assumed for the phase structure of SiC/SiO_x nanocables. Transmission electron microscopy (TEM) (Tecnai-20, PHILIPS Corp.) and high-resolution transmission electron microscopy (HRTEM) (Tecnai F20, FEI Corp.) with energy-dispersive x-ray spectroscopy (EDS) and electron energy loss spectrometer (EELS) were employed to perform the microanalysis of SiC/SiO_x nanocables. Photoluminescence was performed at a fluorescence spectrometer (F4500, Hitachi Corp.) with a resolution of 1.0 nm. Field emission experiments were carried out in a vacuum chamber with a base pressure of about 8×10^{-7} Pa at room temperature. The sample, as a cathode, was attracted to a stainless steel stand with conductive glue. A molybdenum probe of 1 mm^2 in tip area was adopted as an anode. The spacing of 200–1000 μm between these two electrodes was controlled by a stepper. Emission current was measured by a picoammeter (Keithley 485). A ballast resistor of 10 MΩ was used to protect the apparatus against circuit shorting.

III. RESULTS AND DISCUSSION

Figure 1 shows the SEM images of SiC/SiO_x nanocables deposited on the Si(111) substrate at the reaction temperature of 1000 °C for 2 h. High density nanocables are uniformly covered in a large area of 10 mm^2 on the surface of Si(111) substrate, as illustrated in Fig. 1(a). Figures 1(b)–1(d) show SEM images of the nanocables at different magnifications. These nanocables have lengths in the range of several tens to hundreds of micrometers, and the diameter of nanocables is 50–300 nm. Global particles were observed at the tips of the nanocables. Similar products were also observed at reaction temperatures of 1100 and 1200 °C. Figure 2 shows the XRD pattern for the nanowires on Si(111) substrate. Besides the diffraction peaks of Si substrate,[33] (111) and (220) diffraction peaks of β-SiC phase[34] were clearly detected. In addition, a series of weak diffraction peaks of FeSi phase[35] has been observed in the figure, indicating that the β-SiC phase with a small amount of FeSi phase formed on the surface of Si(111) substrate at the above reaction process.

Further sample characterization was carried out using transmission electron microscopy and selected area electron diffraction (SAED). Some white deposits of SiC/SiO_x nano-

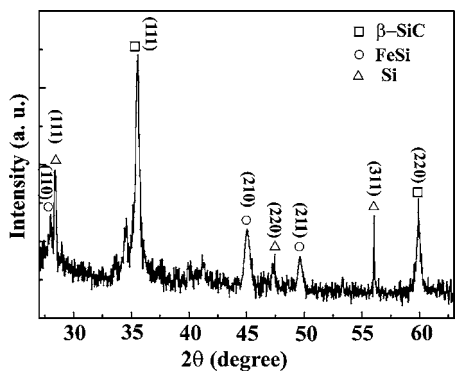

FIG. 2. XRD pattern for the SiC/SiO_x nanocables on Si(111) substrate.

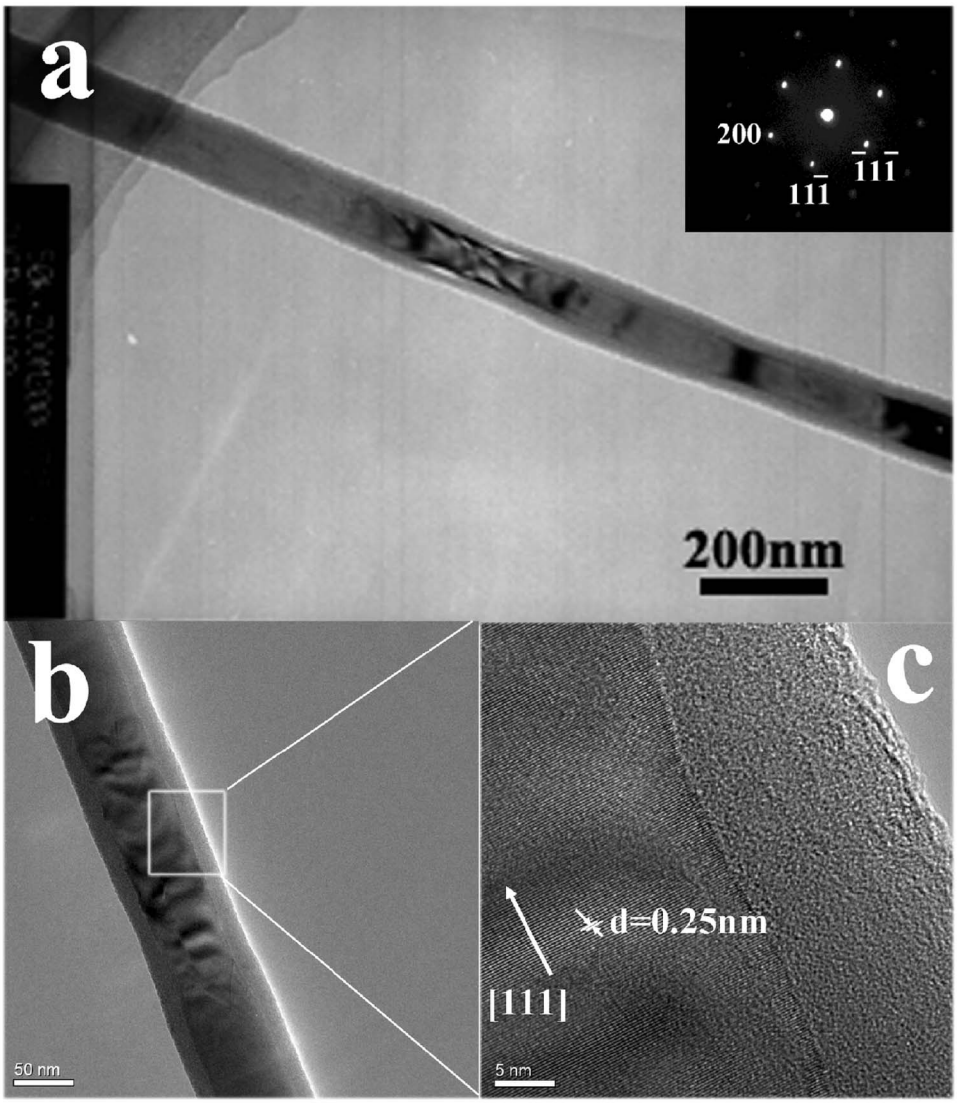

FIG. 3. TEM and HRTEM images taken from a SiC/SiO_x nanocable. (a) A typical TEM image of SiC/SiO_x nanocable and the corresponding SAED pattern (inset). [(b) and (c)] HRTEM images of SiC/SiO_x nanocable, showing a single crystal core and amorphous shell structure.

cables from the Si(111) substrate were peeled off, ultrasonically dispersed in ethanol, and dropped on a copper grid covered with holey carbon film. Figure 3(a) shows a typical TEM image of a nanocable. It can be seen that the nanocable has a core-shell structure, and the diameter of the nanocable is about 100 nm. Electron diffraction was done to determine its structure, as shown in the inset of Fig. 3(a), which suggested that the nanocable is a single crystal. The diffraction pattern can be readily indexed to a cubic β-SiC structure, which is consistent with the results measured by XRD shown in Fig. 2. Figures 3(b) and 3(c) show two HRTEM images of the nanocable. It indicated that the nanocable core is a crystalline phase, while the shell is of amorphous structure. The lattice fringe spacing is 0.250 nm, corresponding to the interspacing of (111) plane of cubic SiC. In order to further investigate the distribution of elements in the nanocable, elemental mappings of carbon, oxygen, and silicon were achieved. Figure 4(a) shows the HRTEM image of the nanocable. Elemental mapping images of carbon, oxygen, and silicon were shown in Figs. 4(b)–4(d). It can be clearly observed that carbon is mainly distributed in the core [Fig. 4(b)], oxygen is mainly located in the outer layer [Fig. 4(c)], and silicon is only detected at the outer layer of nanocable [Fig. 4(d)]. However, the corresponding EDS of the nanocable shows that silicon is distributed throughout the whole nanocable. The reason that the energy-filtering mapping cannot detect silicon at nanocable core is due to the high protrusion of nanocable core compared with the outer layer in the detection limit of the mapping system. EDS analysis also reveals that the Si and O atomic proportion of amorphous sheath is about 1:1.5. So the nanocable consists of a SiC core and an amorphous SiO_x shell.

The vapor-liquid-solid mechanism for the growth of Si and SiC whiskers initiated by a metal catalyst has been suggested by Wanger and Ellis[23] and Urretavizcaya and Lopez:[24] In our experiments, Fe_3O_4 nanoparticles are employed as catalysts to fabricate SiC/SiO_x nanocables. We have also tried to synthesize SiC/SiO_x nanocables without Fe_3O_4 catalysts, which resulted in no one-dimensional SiC nanomaterials on the surface of the Si(111) substrates. Moreover, EDS also detected the existence of iron at the tips of SiC/SiO_x nanocables. This fact suggested that the Fe_3O_4 catalysts play a key role in the formation of SiC/SiO_x nanocables, and a VLS mechanism is the most probable growth mechanism. Here, we give a description for the possible formation of SiC/SiO_x nanocables. Firstly, with the temperature increased

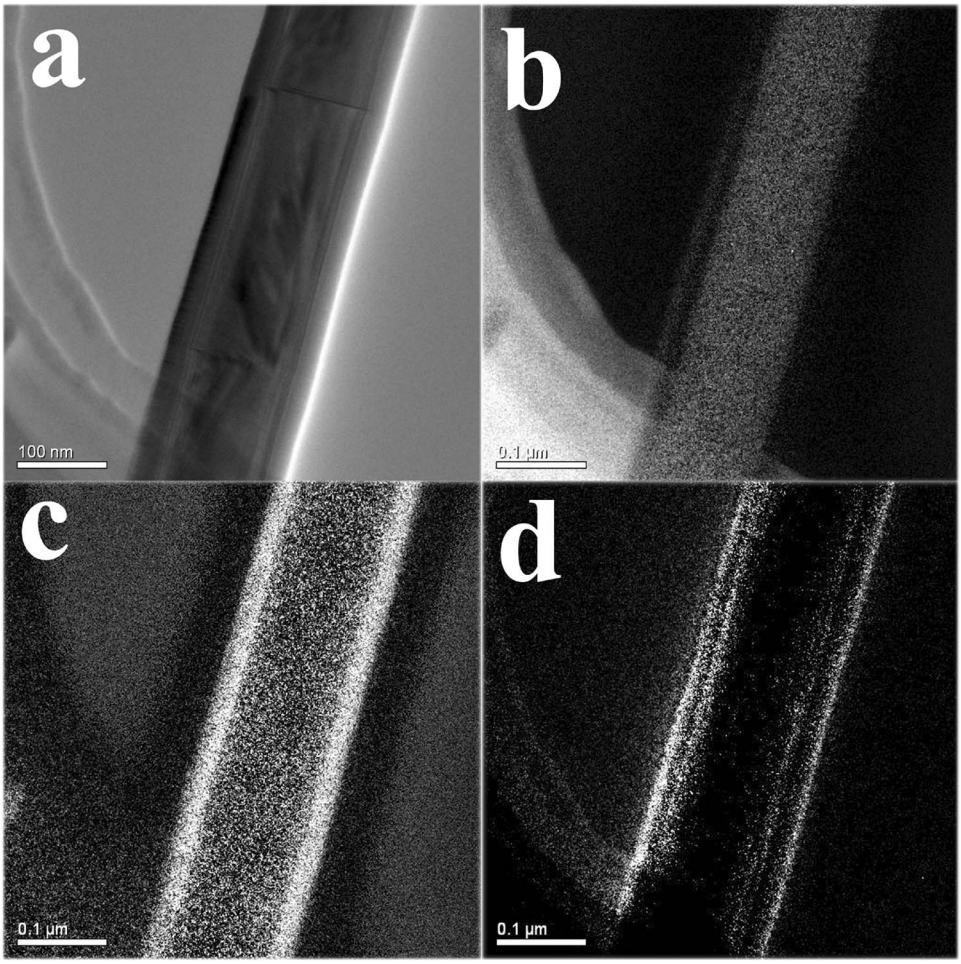

FIG. 4. (a) Bright-field TEM image of SiC/SiO_x nanocable. (b) Elemental mapping of carbon. (b) Elemental mapping of oxygen. (c) Elemental mapping of silicon.

from 400 to 1000 °C, SiO_2 formed on the surface of Si(111) substrate due to the reaction of Si powders with O. Secondly, the carbonthermal reduction of SiO_2 took place,[25]

$$SiO_2 + C \rightarrow SiO + CO. \quad (1)$$

In the meantime, Fe, Si, and C on the surface of Si(111) substrate served as the energetically favored sites for condensation and precipitation of reactant vapors. Fe–Si–C nanoclusters formed on the surface of the Si(111) substrate, which acted as nuclei for the formation of SiC nanowires. Si and C atoms supersaturated in the Fe–Si–C liquid with the increase of SiO and CO pressures. Then the subsequent reaction occurred,[26]

$$SiO + 2C \rightarrow SiC + CO, \quad (2)$$

$$2SiO + 3C \rightarrow 2SiC + CO_2. \quad (3)$$

With the procession of the above two reactions, a large amount of β-SiC nanowires formed. Finally, the SiC nanowires may be oxidized to form an amorphous SiO_x shell, or the unreacted SiO and O_2 took place to form the amorphous silicon oxide, then deposited on the SiC nanowires.[21]

Figure 5 shows the room-temperature photoluminescence spectrum of SiC/SiO_x nanocables under the 250 nm ultraviolet fluorescent light excitation. Two broad PL emission peaks are clearly observed at the center wavelengths of about 390 and 460 nm. The former emission peak results from the effect of the oxygen discrepancy in the SiO_x amorphous layer.[13] The emission peak centered at 460 nm may be ascribed to the blue emission luminescence from SiC nanowires. The latter emission peak has a blueshift compared with the previous studies on the PL of bulk SiC, which may be the effect of quantum confinement in the synthesized SiC nanowires.[27] The ultraviolet-blue emission properties of SiC/SiO_x nanocables are of significant interest for their potential ultraviolet-blue emitting device applications.

Figure 6(a) shows the current density versus the electric field (J-V) characteristics for SiC/SiO_x nanocables at the vacuum gaps ranging from 200 to 1000 μm. The electric fields at the current densities of 10 $\mu A/cm^2$ and 10 mA/cm^2

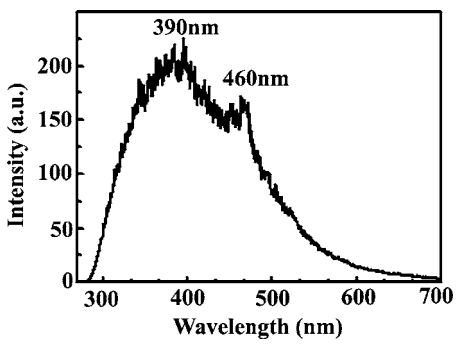

FIG. 5. The room-temperature photoluminescence spectrum of SiC/SiO_x nanocables under the 250 nm ultraviolet fluorescent light excitation.

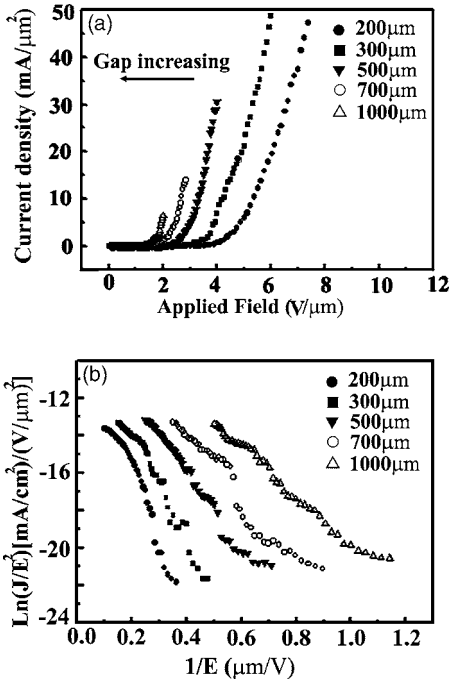

FIG. 6. (a) Field emission *J-V* curves of SiC/SiO_x nanocables with the vacuum gaps from 200 to 1000 μm and (b) corresponding FN plots.

are defined as the turn-on and the threshold electric fields, respectively. With a vacuum gap of 200 μm, low turn-on and threshold electric fields of 3.2 and 5.3 V/μm were observed for the SiC/SiO_x nanocables. Emission current density was increased to 50 mA/cm^2, and no saturation tendency was seen at the electric field of 7.2 V/μm. When the vacuum gap was increased from 200 to 1000 μm, the threshold electric field decreased monotonously from 5.3 to 2.3 V/μm, while the voltage applied on the two electrodes increased from about 1150 to 2300 V. The threshold electric field value is relatively low when compared to those of SiC nanowires,[16] SiC nanorods,[6] and SiC nanoneedles,[28] and close to SiC nanowires with carbon and BN sheath.[29,30] Compared with conventional SiC nanowires, it is suggested that there are three reasons for enhanced field emission properties of SiC/SiO_x nanocables. Firstly, high density nanowires have more efficient electron emitting sites, leading to better field emission properties. Secondly, the wide-band-gap SiO_x shell layer has a small electron affinity (0.6–0.8 eV), which can enhance the field emission of SiC emitters. Similar results have also been observed for the SiO_2-coated SiC nanowires by Ryu *et al.*[7] Thirdly, it is also believed that the field enhancement β, which reflects the ability of the emitters to enhance the local electric field at the tip, is strongly dependent on the geometry of materials.[31] Shen *et al.*[15] reported that bamboolike SiC nanowires with a high aspect ratio have a better field emission than SiC nanowires with even diameter and lengths. The present SiC/SiO_x nanocables have a large diameter range of 50–300 nm and length ranges of tens to up to several hundred micrometers. This means that the present SiC/SiO_x nanocables have a high aspect ratio, which contributes to the geometry enhancement factor and greatly enhances the electron emission.

The *J-V* relationship was analyzed by the Fowler-Nordheim (FN) theory for metal, which was described as Eq. (4),[32]

$$J = A\left(\frac{\beta^2 E^2}{\phi}\right)\exp\left(-\frac{B\phi^{3/2}}{\beta E}\right). \tag{4}$$

In the equation, J is the emission current intensity, E is the electric field, ϕ is the work function, and A and B are constants. Figure 6(b) shows the corresponding FN plots of SiC/SiO_x nanocables at the different vacuum gaps from 200 to 1000 μm. It exhibits approximately linear behaviors in the measured range of 0.1–1.2 μm/V, indicating that the FN theory perfectly fits the field emission behavior of our samples, and the field emission of SiC/SiO_x nanocables should be a barrier-tunneling, quantum-mechanical process.[16]

IV. CONCLUSIONS

Large scale, high yield SiC/SiO_x nanocables have been synthesized by using a simple and low-cost chemical vapor deposition method. The SiC/SiO_x nanocables grew by a two-step raising temperature process based on the VLS mechanism. These nanocables consist of a 50–300 nm single-crystalline β-SiC core and a 10–20 nm amorphous SiO_x shell. The length is in the range of several tens to hundreds of micrometers. Two broad PL peaks at 390 and 460 nm were observed at room temperature. The results of field emission measurement show the low turn-on and threshold electric fields of 3.2 and 5.3 V/μm at the vacuum gap of 200 μm, respectively. When the vacuum gap was increased to 1000 μm, the turn-on and threshold electric fields were decreased to 1.1 and 2.3 V/μm, respectively.

ACKNOWLEDGMENTS

This work was supported in part by the National 863 and 973 projects, the National Science Foundation of China (Grant No. 60571045), and the China Postdoctoral Science Foundation.

[1] S. Iijima, Nature (London) **354**, 56 (1991).
[2] Y. N. Xia, P. D. Yang, Y. G. Sun, T. Y. Wu, B. Mayers, Y. D. Yin, F. Kim, and H. Q. Yan, Adv. Mater. (Weinheim, Ger.) **15**, 353 (2003).
[3] A. Fissel, B. Schroter, and W. Richter, Appl. Phys. Lett. **66**, 3182 (1995).
[4] Y. Morisada, M. Maeda, T. Shibayanagi, and Y. Miyamoto, J. Am. Ceram. Soc. **87**, 804 (2004).
[5] E. W. Wong, P. E. Shaehan, and C. M. Lieber, Science **277**, 1971 (1995).
[6] S. Z. Deng *et al.*, Appl. Phys. Lett. **89**, 023118 (2006).
[7] Y. W. Ryu, Y. J. Tak, and K. Yong, Nanotechnology **16**, S370 (2005).
[8] H. Dai, E. W. Wong, Y. Z. Lu, S. S. Fan, and C. M. Lieber, Nature (London) **375**, 769 (1995).
[9] W. Han, Chem. Phys. Lett. **265**, 374 (1997).
[10] Y. Zhang, T. Ichihashi, E. Landree, F. Nihey, and S. Iijima, Science **285**, 1719 (1999).
[11] J. Q. Hu *et al.*, J. Phys. Chem. B **104**, 5251 (2000).
[12] Z. J. Li, H. J. Li, X. L. Chen, A. L. Meng, K. Z. Li, Y. O. Xu, and L. Dai, Appl. Phys. A: Mater. Sci. Process. **76**, 637 (2003).
[13] H. K. Seong, H. J. Choi, S. K. Lee, J. I. Lee, and D. J. Choi, Appl. Phys. Lett. **85**, 1256 (2004).
[14] H. Lai *et al.*, Appl. Phys. Lett. **76**, 294 (2000).
[15] G. Z. Shen, Y. Bando, C. H. Ye, B. D. Liu, and D. Golberg, Nanotechnology **17**, 3468 (2006).
[16] K. W. Wong, X. T. Zhou, C. K. Frederick, H. L. Lai, C. S. Lee, and S. T. Lee, Appl. Phys. Lett. **75**, 2918 (1999).

[17]J. Wei, K. Z. Li, H. J. Li, Q. G. Fu, and L. Zhang, Mater. Chem. Phys. **95**, 140 (2006).
[18]W. M. Zhou, Z. X. Yang, F. Zhu, and Y. F. Zhang, Physica E (Amsterdam) **31**, 9 (2006).
[19]J. W. Liu, D. Y. Zhong, F. Q. Xie, M. Sun, E. E. G. Wang, and W. X. Liu, Chem. Phys. Lett. **348**, 357 (2001).
[20]X. M. Liu and K. F. Yao, Nanotechnology **16**, 2932 (2005).
[21]T. Seeger, P. Redlich, and M. Ruffhle, Adv. Mater. (Weinheim, Ger.) **12**, 279 (2000).
[22]T. Z. Yang *et al.*, J. Phys. Chem. B **109**, 23233 (2005).
[23]R. S. Wanger and W. C. Ellis, Trans. Metall. Soc. AIME **233**, 1053 (1965).
[24]G. Urretavizcaya and G. P. Lopez, J. Mater. Res. **9**, 2981 (1994).
[25]W. Q. Han, S. S. Fan, Q. Q. Li, B. L. Gu., and D. P. Yu, Chem. Phys. Lett. **265**, 374 (1997).
[26]C. H. Liang, G. W. Meng, L. D. Zhang, Y. C. Wu, and Z. Cui, Chem. Phys. Lett. **329**, 323 (2000).
[27]H. J. Choi *et al.*, J. Phys. Chem. B **107**, 8721 (2003).
[28]Z. S. Wu, S. Z. Deng, N. S. Xu, J. Chen, J. Zhou, and J. Chen, Appl. Phys. Lett. **80**, 3928 (2002).
[29]C. C. Tang and Y. Bando, Appl. Phys. Lett. **83**, 659 (2003).
[30]Y. H. Ryu, B. T. Park, Y. H. Song, and K. J. Yong, J. Cryst. Growth **271**, 99 (2004).
[31]C. J. Lee, T. J. Lee, S. C. Lyu, Y. Zhang, H. Ruh, and H. J. Lee, Appl. Phys. Lett. **81**, 3648 (2002).
[32]R. H. Fowler and L. W. Nordheim, Proc. R. Soc. London, Ser. A **119**, 173 (1928).
[33]JCPDS Card No. 80-0018 (unpublished).
[34]JCPDS Card No. 74-2307 (unpublished).
[35]JCPDS Card No. 86-0793 (unpublished).